1 **Extracellular vesicles from monocyte/platelet aggregates modulate human**

2 **atherosclerotic plaque responses**

3

4 **Authors** Oggero S[1], M.Sc., de Gaetano M[2], Ph.D., Marcone S[3], Ph.D., Barry M[4],

5 M.D., Montero-Melendez T[1,5], Ph.D., Cooper D.[1,5], Ph.D., Norling L V[1,5], Ph.D.,

6 Brennan E P[2], Ph.D., Godson G[2], Ph.D., Perretti M[1,5], Ph.D.

7 **Institution:**

8 [1] William Harvey Research Institute, Barts and the London School of Medicine,

9 Queen Mary University of London, London, United Kingdom.

10 [2] Diabetes Complications Research Centre, Conway Institute, & School of Medicine

11 University College Dublin, Dublin, Ireland.

12 [3] Trinity Translational Medicine Institute, Trinity College Dublin, Dublin, Ireland.

13 [4] Department of Vascular Surgery, St. Vincent's University Hospital, Dublin, Ireland.

14 [5] Centre for inflammation and Therapeutic Innovation, Queen Mary University of

15 London, London, United Kingdom.

16 **Running title:** Monocyte EVs in atherosclerosis.

17 **Correspondence to:**

18 Mauro Perretti, The William Harvey Research Institute, Barts and the London School

19 of Medicine, Charterhouse Square, London, EC1M 6BQ, United Kingdom.

20 Tel: +44-2078828782; Fax:+44-2078826065; E-mail: m.perretti@qmul.ac.uk.

21

22 **Characters count:** 54784

23

24 **Subject codes:** Inflammation, Atherosclerosis, Coronary Artery Disease, Cell

25 biology.

Oggero et al., v1

Abstract

In atherosclerosis, a chronic disease characterized by lipid accumulation, fibrosis and vascular inflammation, extracellular vesicles (EVs) are emerging as key players in different stages of disease development. Here we provide evidence that EVs released by mixed aggregates of monocytes and platelets in response to TNF-α are both CD14+ and CD41+. Tempering platelet activation with Iloprost™ impacted the quality and quantity of EV produced. Proteomics of EVs from cells activated with TNF-α alone or in presence Iloprost™ revealed distinct proteome, with selective hits like gelsolin. EVs from TNF-α stimulated monocytes augmented release of cytokines, and modulated more than 500 proteins by proteomics, when added to human atherosclerotic plaques. In contrast, EVs generated by TNF-α and Iloprost™ produced minimal plaque activation. In conclusion, attenuating platelet activation has an effect on EV composition released from monocyte/platelet aggregates with downstream modulation of their pro-inflammatory actions and contribution to the development and progression of atherosclerosis.

Keywords: monocyte/platelet aggregates, vascular inflammation, proteomics.

Abbreviations: ELISA: enzyme linked immunoassay; EV: extracellular vesicle; FBS: foetal bovine serum; FMO: fluorescence minus one; LC-MS: liquid chromatography-mass spectrometry; PA: pathways analysis; PAF: Platelet Activator Factor; PBMCs: peripheral blood mononuclear cells; PBS: phosphate buffer saline; PRP: platelet rich plasma; T-PBS: PBS with 0.1% Triton; TNF-α: Tumour Necrosis Factor-α.

1

Introduction

Extracellular vesicles (EVs) are cell-borne particles that contain a complex biological cargo composed of nucleic acids, proteins and lipids. Firstly described by Wolf in 1967, EVs were reported to have prothrombotic functions (1) and proposed to be a way for cells to dispose of unnecessary products (2). Since then, EVs have been ascribed extended properties impacting on both pathological and physiological processes, including modulation of adaptive immune response (3), tumour metastasis and growth (4), and coagulation cascade (5).

The majority of work conducted so far with EVs has focused on identifying the markers of cell of origin they bear; however, using neutrophil-derived EVs as prototypes, we proposed that their composition and hence properties would vary to reflect the environment surrounding the cell source (6). This study helped to develop the concept of EV heterogeneity (7): EVs mirror the activation state of their cell of origin through specific enrichment or presence of given proteins, lipids and nucleic acids, affecting in this manner their biological properties. For example, the procoagulant property of endothelial cell-derived EV is largely dependent on both the exposure of tissue factor and phosphatidylserine on the particle surface (8,9), while EV-mediated induction of endothelial cell proliferation is mainly tissue factor-dependent (10).

Atherosclerosis is the most prominent and common cause of cardiovascular diseases responsible for ~50% of all deaths in Europe (11). Complications of atherosclerosis, especially acute coronary syndromes, have been linked to rupture of vulnerable lesions, causing atherothrombosis and vessel occlusion. In the

77 pathogenesis of atherosclerosis, most of the cellular and molecular events including

78 endothelial dysfunction, platelets activation and monocyte and macrophage

79 accumulation, have been characterized (12), yet effective prevention of

80 atherosclerosis and adverse cardiovascular events are still needed. Thus, studying

81 the lesion biology is essential for growing our knowledge on the pathophysiology of

82 atherosclerosis and to allow identification and development of novel therapeutic

83 strategies. In this context, the possible implication of EVs in promoting and

84 progressing this pathology is a recently explored field.

85

86 There is evidence for EVs to cause endothelial dysfunction, vascular calcification,

87 unstable plaque progression, rupture and thrombus formation (13). Regarding

88 plaque formation and destabilization, studies have focused on plaque-released EVs.

89 For example, atherosclerotic plaque EVs expressed surface antigens of leukocyte

90 origin (including major histocompatibility complex classes I and II), and promoted T-

91 cell proliferation (14). In terms of EVs effects once added to the plaque, there is *in*

92 *vivo* evidence for monocyte EVs to promote leucocyte adhesion to post-capillary

93 venules and T-cell infiltration in atherosclerotic plaques (15). The majority of these

94 studies have been conducted with murine models and *in vitro* cellular assays.

95 However a better assessment of the inflammatory processes in human

96 atherosclerosis can be attained through organ culture approaches, rather than using

97 less complex experimental settings.

98

99 Here, we characterise human monocyte-derived EVs particularly in presence of

100 platelets, to mimic a vascular inflammatory status, and define the composition of

101 these EVs and their biological function once added to human atherosclerotic

102   plaques, observing a positive feed-forward mechanism fuelling inflammation and

103   possibly instability. Intriguingly, attenuating platelet activation has an impact on EV

104   composition and a functional effect on modulating the reactivity of the atherosclerotic

105   plaque.

106

107

plaques, observing a positive feed-forward mechanism fuelling inflammation and

108 **Results.**

109 <u>Monocyte-derived EVs are regulated by aggregation with platelets.</u> After preparation

110 of an enriched population of monocytes from human blood using negative selection

111 procedure, flow cytometry analysis demonstrated a high degree of monocyte/platelet

112 aggregates whereby 56.5±5.1% of CD14+ events were also positive for CD41+, the

113 platelet marker (n=10; Fig. 1a and b). In order to determine whether platelet-

114 monocyte interactions were dependent on platelets activation, we introduced Iloprost

115 a potent analogue of prostacyclin in our isolation protocol. Addition of Iloprost during

116 the isolation procedure did not impact on the formation of these aggregates (Fig. 1c),

117 a phenomenon also visualised by ImageStream™ (Fig. 1f). A similar outcome was

118 observed when cells were purified using the Histopaque low density gradient

119 protocol (Fig. 1c).

120

121 A degree of monocyte and platelet activation consequent to the purification

122 procedure was confirmed by transient cell surface expression of P-selectin and

123 PSGL-1 compared when cells were purified using the Histopaque low density

124 gradient protocol (Fig. 1d and e). EV-free monocyte supernatants were analysed to

125 assess activation status, and an increase in all cytokine and chemokine levels were

126 detected with TNF-α treatment with no significant modulation by the prostacyclin

127 analogue (Fig S1).

128 **Figure 1. Iloprost controls platelet but not monocyte activation.** Whole blood (WB) or
129 monocytes isolated using the RosetteSep purification protocol were incubated with or without 1
130 µM Iloprost (PGI$_2$). CD14 and CD41 were used as markers for monocytes and platelets,
131 respectively, for flow cytometry and Imagestream™ analyses. (a) Dotplot graph showing
132 monocyte (CD14+) and platelet (CD41+) immunostaining to reveal presence of aggregates
133 (double positive events). (b) Percentages of CD14+ (monocytes), CD41+ (platelets),
134 CD14+/CD41+ double positive (aggregates) events. Data are mean ± SEM of n=10 distinct cell
135 preparations. Representative of n=10 distinct cell preparations. (c) Proportion of aggregates as
136 analysed by Imagestream™ comparing Whole blood (WB) cells with purified monocytes in the
137 presence or absence of Iloprost (*p<0.05, **p<0.01, ***p< 0.001; one-way ANOVA post
138 Bonferroni test, mean ± SEM, n=5 distinct preparations). (d) P-selectin expression of

139 monocyte/platelets aggregates following presence or absence of Iloprost compared to WB
140 cells. Data are mean ± SEM of n=4 distinct cell preparations. (e) PSLG-1 expression of
141 monocyte/platelet aggregates upon addition or not of Iloprost following presence or absence of
142 Iloprost compared to WB cells. Data are mean ± SEM of n=4 distinct cell preparations. (f)
143 Visualization of monocyte/platelet aggregates as identified by ImageStream™. Representative
144 of n=5 distinct cell preparations.

145

146 These data indicate that monocyte isolation leads to immune cells carrying platelets

147 and that Iloprost addition does not affect the extent of this interaction. Since

148 monocyte/platelet aggregates are typical of several cardiovascular settings, including

149 atherosclerosis (see Discussion), we decided to exploit this enriched monocyte

150 preparation herein obtained to study formation and properties of EVs generated in

151 these cell-to-cell crosstalk settings.

152

153 For deep analysis of EVs, we implemented a validated protocol where fluorescence

154 triggering of EVs (labelled with BODIPY-FITC) allows a better identification by

155 ImageStream™(Headland et al. 2015). Using a double gating strategy for staining

156 with CD14+ and CD41+, EVs from platelets (CD41+/CD14-; ~15%), monocytes

157 (CD41-/CD14+; ~60%) and a subset bearing both markers (CD41+/CD14+; ~7.5%)

158 were identified, both in presence and absence of TNF-α and Iloprost (Fig. 2a). TNF-α

159 addition to monocytes almost doubled the number of total EVs compared with

160 unstimulated cells (n=5, P<0.01) (Fig. 2b). Addition of Iloprost did not affect basal EV

161 numbers (Fig. 2b). Similar results were obtained for total CD14+ EV, however

162 addition of Iloprost significantly reduced (~40%) the proportion and number of both

163 CD41+/CD14- and CD14+/CD41+ EVs as quantified in response to TNF-α

164 stimulation (Fig. 2c-e). When the cellular preparations were stimulated with PAF, a

165 known activator of platelets as well as of monocytes, a larger number of EVs were

166 produced with a higher proportion of CD14+/CD41+ events (1/5 of total CD14+

167 events); this time Iloprost afforded a marked reduction of all EV subset values (Fig.

168   S2). Thus while Iloprost did not affect formation of monocyte/platelet aggregates and

169   exerted selective inhibition on TNF-α stimulated EV numbers and phenotypes, it

170   markedly affected PAF stimulation indicating high efficacy in reducing platelet and

171   monocyte activation, regulating mainly the release of platelet EVs (CD41+) and

172   CD14+/D41+ double positive EVs.

173   **Figure 2. Characterization of monocyte/platelet derived EVs.** Monocytes were isolated
174   using the RosetteSep purification protocol. Cells (1×10^6/ml) were incubated with vehicle (V) or
175   TNF-α (50 ng/ml), in presence or absence of Iloprost (1 µM; PGI_2) for 60 min. **(**a)
176   ImageStream™ analysis of the vesicle showing quadrant selections, FMOs and representative
177   images following staining for anti-CD14 or anti-CD41. EV generation in cell-free supernatants
178   was quantified following Bodipy staining for total vesicles (b); monocyte CD14+ EVs (c); platelet
179   CD41+ EVs (d) and double positive CD14+/CD41+ vesicles (e). (*$p<0.05$, **$p<0.01$, ***$p<$
180   0.001; one-way ANOVA post Bonferroni test, mean ± SEM, n=5 distinct preparations). (f)
181   Visualization of CD14+ (top panel), CD41+ (middle panel) and CD14/CD41 double positive
182   (bottom panel) EVs by ImageStream™.
183

184   The physical characteristics of EVs were studied by nanoparticle tracking analysis.

185   This set of experiments demonstrated that vesicles produced in these settings

186   ranged between 50 and 500 nm in diameter (Fig. S3); addition of Iloprost had

187   modest or nihil effect on the physical characteristics of the EV samples. All

188   preparations of EVs displayed similar size mean and mode regardless of the

189   stimulating agent applied or presence of Iloprost (Fig. S3).

190

191   EVs differentially activate HUVEC. Since EVs from different cellular sources can

192   activate endothelial cells (17,18), a major cellular player in blood vessel

193   angiogenesis and plaque formation (19,20), we queried whether EVs derived from

194   monocyte/platelet aggregates could impact on HUVEC reactivity. An overnight

195   protocol was applied, testing initially a concentration-range of 1 to 20 EVs per

196   endothelial cell. These experiments combined with published data (17,21) indicated

197   that a ratio of 10 EVs/Cell was optimal for our experimental approach. Indeed,

198   microscopy imaging showed changes in HUVEC morphology after incubation with

199 EVs isolated from monocyte stimulated with TNF-α (Fig. 3a). Furthermore cells

200 showed a significant uptake of these EVs after 24 hour incubation (Fig. 3b). Next we

201 quantified markers of cell activation.

202

203 Flow Cytometry analysis revealed that expression of ICAM-1 and VCAM-1 was

204 significantly upregulated when cells were treated with 10 ng/mL of TNF-α as positive

205 control. Furthermore, similar increases were recorded when HUVEC were stimulated

206 with EVs isolated from monocytes enriched preparations incubated with TNF-α. Of

207 interest, ICAM-1 levels were no modified at all following incubation with EVs isolated

208 from Iloprost and TNF-α stimulated monocytes (Fig. 3c). When similar experiments

209 were repeated with the same concentrations ($10x10^6$) of platelet EVs, isolated from

210 cells in both stimulated (TNF-α) or in resting conditions, expression of either ICAM-1

211 or VCAM-1 was not modified, suggesting a synergistic role of monocyte/platelet

212 aggregates in releasing functional EVs upon TNF-α stimulation (Fig. S4). Of

213 relevance, only negligible amounts of residual TNF-α were detected in any of the

214 vesicle preparations used (Fig. S5).

215

216 Cytokine measurements of HUVEC supernatants was then conducted. Cell

217 incubation with EVs released by monocytes stimulated with TNF-α augmented

218 concentrations of GM-CSF, IL-6 and IL-8 to a significant degree (Fig. 3d-f). When

219 EVs were produced in presence of Iloprost, a lower regulation of these three

220 cytokines was quantified (Fig. 3-f). These data together suggested a different pro-

221 inflammatory effect of EVs generated from enriched monocyte preparations in

222 response to several conditions chosen to mimic vascular inflammation.

223 **Figure 3. Monocyte/platelet EVs activate HUVEC *in vitro*.** Monocyte were obtained as in
224 Figure 2 and incubated with vehicle (V) or TNF-α (50 ng/ml), in presence or absence of

225   Iloprost (1 µM; PGI$_2$) for 60 min. HUVEC were incubated with the reported EVs (10x10^6/ml)
226   overnight. Cells were stained for flow cytomentry analysis and and supernatants were
227   collected and analysed for cytokine release. (a) Representative microscopic image of
228   HUVEC after treatment monocyte EVs from vehicle-incubated monocyte or TNF-α
229   stimulated cells. (b) Confocal images of the uptake by HUVEC stained with Phalloidin (red)
230   after 24 hours of BODIPY labelled EV isolated from TNF-α stimulated cells (green/white
231   arrows). (c) Quantification of ICAM-1 and VCAM-1 expression (MFI units) in HUVEC treated
232   with different subsets of monocyte derived EVs. (d) Quantification of GMCSF, IL-6 and IL-8
233   levels by ELISA. (*p<0.05, **p<0.01, ***p< 0.001; one-way ANOVA post Bonferroni test,
234   mean ± SEM of n=5 cell preparation incubated with distinct EV preparations from different
235   donor cells).

236

237   <u>EV triggers differential activation of human atherosclerotic plaque.</u> Having confirmed

238   that EVs derived from monocyte/platelet aggregates can activate endothelial cells,

239   we tested if they might be a functional determinant in atherosclerosis. Thus, we

240   assessed their function on an atherosclerotic plaque using an *ex-vivo* organ culture

241   protocol (Fig. 4a-b). Herein we compared an overnight incubation with EVs

242   generated from different cellular activation protocols, using the same concentration

243   of EVs, as described in the previous section, to resemble vascular inflammation.

244   Then, we quantified cytokines and proteins released in the supernatants from the

245   plaque fragments.

246

247   Cytokine multiplex analyses revealed that treatment of the plaque with EVs released

248   by monocytes stimulated with TNF-α, augmented concentrations of TNF-α, IL-6, IL-

249   13, IFN-γ and GM-CSF in the culture media (Fig. 4c and Supplementary Table S2).

250   As mentioned already above only negligible amounts of residual TNF-α were

251   detected in any of the vesicle preparations used (Fig. S5). When EVs were

252   generated in the presence of Iloprost, a much milder regulation of the general

253   cytokine response was noted (Fig. 4c). These findings seemed to confirm the

254   acquisition of a pro-inflammatory phenotype of EVs not only *in vitro* but also *ex vivo*

255   when monocytes enriched preparation were stimulated with TNF-α. Such an effect

256 was markedly attenuated when EVs were generated by Iloprost+TNF-α treatment, a

257 finding corroborated by further quantification of IL-6 and IL-13 in the supernatants.

258 (Fig. 4d,e). Of importance, the use of 0.1% FBS to enable plaques fragments viability

259 did not affect the experimental outcome.

260 **Figure 4. Monocyte/platelet EVs activate human atherosclerotic plaque ex-vivo.**
261 Monocyte were obtained as in Figure 2 and incubated with vehicle (V) or TNF-α (50 ng/ml),
262 in presence or absence of Iloprost (1 µM; PGI2) for 60 min. Human atherosclerotic plaque
263 fragments were incubated with the reported EVs (10x106/ml) overnight. Supernatants were
264 collected and used for ELISA analysis. (a,b) Representative images of human femoral
265 plaque and fragment incubation. (c) Heat map analysis showing qualitative modulation of
266 cytokine release (linear scale bar). (d,e) Quantification of IL-6 and IL-13 levels by ELISA.
267 (*$p<0.05$, **$p<0.01$, ***$p< 0.001$; one-way ANOVA post Bonferroni test, mean ± SEM of n=5
268 plaques incubated with distinct EV preparations from different donor cells).
269

270 To acquire a view of the broader effects of these EVs on plaque reactivity, tissue

271 conditioned media were analysed by proteomics. In total, 654 proteins were

272 identified in human plaque supernatants as reported in Table S3. Subsequently, we

273 performed statistical analysis in order to determine proteins differentially secreted

274 between plaques treated with different EVs subsets as compared to the untreated

275 plaque. In total, 52 proteins resulted significantly modulated with the majority of

276 these proteins (13) being uniquely modulated when the plaque was treated with

277 TNF-α-stimulated monocyte/platelet aggregates EVs. Treatment of plaque with EVs

278 from unstimulated cells (vehicle) produced a limited response with 6 significant

279 proteins being modulated. Both EVs from Iloprost (PGI$_2$) and Iloprost+TNF-α

280 monocytes resulted in the modulation of the release of a different set of 8 unique

281 proteins (Fig. 5a). Only 3 proteins were common between all the groups (Fig. 5a):

282 guanine nucleotide-binding protein subunit beta-2-like 1 (GNBL1; a regulator of

283 several signalling pathways), Serpin B6 (SERPINB6; natural inhibitor of serine

284 proteinases) and Voltage-dependent anion-selective channel protein 1 (VDAC1; a

285 protein that forms a channel through plasma membrane). Details of the proteins

286   identified in this analysis are reported in Table S4. As shown in Figure 5a, functional

287   enrichment analysis of the modulated proteins mapped to distinct cellular functions

288   including immune system, neutrophil degranulation and extracellular matrix

289   organization. Of interest, plaque fragments treatment with EVs isolated from TNF-α

290   stimulated monocytes not only increased the overall number of modulated proteins

291   but a higher number of proteins involved in these functions emerged as well.

292

293   Prompted by the distinct phenotypic response of the plaque to different EVs subsets,

294   we performed a targeted analysis directly comparing plaque treated with TNF-α EVs

295   and Iloprost+TNF-α EVs: this analysis revealed a set of 15 modulated proteins as

296   reported in Figure 5b. Of these, nine proteins were downregulated while six proteins

297   were upregulated (Fig. 5b).STRING network analysis showed an enrichment in 6

298   proteins involved in extracellular matrix reorganization (Fig. 5c), a process which is

299   crucial in vascular remodelling and atherosclerotic plaque formation. Fibulin (FBLN2)

300   was consistently upregulated from plaques treated with TNF-α EVs but not with

301   Iloprost+TNF-α EVs. This protein is emerging as a major effector in cardiac fibrosis

302   and tissue remodelling (see Discussion) suggesting it may play a pivotal role in

303   plaque activation and likely destabilization following incubation with TNF-α EVs.

304   Conversely, Gelsolin (GSN) is a protein involved in actin filament assembly and

305   organization (22), hence described to maintain the cytoskeleton structure in arteries

306   (see Discussion), showed an opposite modulation.

307   **Figure 5. Modulation of secreted proteins from human atherosclerotic plaques by**
308   **monocyte/platelet EVs.** Monocyte were obtained as in Figure 2 and incubated with vehicle
309   (V) or TNF-α (50 ng/ml), in presence or absence of Iloprost (1 µM; PGI$_2$) for 60 min. Human
310   atherosclerotic plaque fragments were incubated with the indicated EV subsets (10x10^6/ml)
311   overnight and proteomic   conducted on supernatants. (a) Venn Diagram and related
312   reactome pathway enrichment analysis obtained by PANTHER software clustering the
313   significantly modulated proteins (p<0.05) by the EV treatments as indicated. (b) Hierarchical
314   clustering heatmap identifying the 15 secreted proteins that were significantly modulated
315   when comparing TNF-α EVs versus TNF-α+PGI$_2$ EVs (p<0.05). Red represents up-regulated

316 proteins while blue depicts down-regulated proteins. (c) Protein-Protein interaction network
317 of the 15 proteins obtained by STRING: network nodes represent proteins; network edges
318 indicate the strength of data support; proteins associated with "extracellular matrix
319 organization" pathway are highlighted in red.

320

321 <u>Characterization of monocyte EV subsets revealed differential protein expression</u>

322 <u>associated with regulation of vascular inflammation and plaque formation.</u> The

323 experimental data presented so far are indicative of different pharmacodynamics

324 properties produced by EVs obtained with TNF-α-treated monocytes compared to

325 vesicles generated following treatment with Iloprost+TNF-α. In order to verify if these

326 effects were mediated by a differential EVs composition we performed a proteomic

327 characterization of TNF-α and Iloprost+TNF-α EVs. We identified 681 proteins in

328 EVs by LS-MS/MS (Table S5), of which 32 proteins were significantly altered

329 (p<0.05) when comparing TNF-α EVs to Iloprost+TNF-α EVs. (Fig. 6a): of these, 19

330 proteins were upregulated and 13 downregulated following cell incubation with

331 Iloprost (Fig. 6b). Moreover, proteins uniquely expressed were also identified: 10

332 proteins for TNF-α EVs and only two for Iloprost+TNF-α EVs (Fig. 6a). Of interest,

333 we detected Annexin A1, which is a faithful marker for membrane-spawn vesicles

334 (23). Gelsolin (GSN) was identified as an interesting protein which was augmented in

335 Iloprost+TNF-α EVs; this protein was also identified in the plaque proteomic analysis

336 (see previous section). However, Fibulin was not a hit identified by this analysis

337 (Table S5), while being regulated in the plaque proteome as discussed above. Next,

338 and to further validate these data, we confirmed the relative abundance of a selected

339 group of proteins by Western blotting and Imaging flow cytometry.

340

341 To this end, equal numbers of monocyte/platelet EVs of each subset were loaded

342 and immunostained for GSN, ANXA1, HSPB1 employing ATCB as a loading control.

343   The blots confirmed that GSN was enriched in Iloprost+TNF-α EVs (Fig. 6c),

344   whereas HSPB1 and ANXA1 were mildly regulated across the two EV subsets (Fig.

345   6d), again confirming the proteomics results. ImageStream analyses revealed that

346   GSN and ANXA1 were also detected of the surface of the EVs (Fig. 6e), establishing

347   again the selective enrichment of GNS in EVs isolated from monocytes stimulated

348   with Iloprost and TNF-α (Fig. 6f), but not major changes for ANXA1. When CD41+

349   EVs were analysed, GSN+ EVs were 46.1±1.94% in TNF-α EVs and 63.4 ± 2.15% in

350   the Iloprost+TNF-α EV group (mean ± SEM, n=3 distinct preparations).

351   **Figure 6. Proteomic analysis of monocyte/platelet EVs.**   Monocyte were obtained as in
352   Figure 2 and incubated with TNF-α (50 ng/ml), in presence or absence of Iloprost (1 µM;
353   PGI$_2$) for 60 min, prior to EV purification. Targeted analysis highlighting differences between
354   TNF-α and TNF-α+PGI$_2$ EVs identified 33 proteins that were significantly altered (Table S5).
355   (a) Venn diagram showing the proteins that are differentially expressed between TNF-α
356   versus PGI$_2$+TNF-α EVs. In the intersection of the diagram are reported the proteins there
357   are significantly altered between the two EVs populations (p<0.05, red represents up-
358   regulated proteins while blue depicts down-regulated proteins in TNF-α+ PGI2 EVs). In
359   black, we identify proteins that are uniquely expressed in either EVs population. (b)
360   Hierarchical clustering heatmap of differentially expressed proteins (centre of Venn diagram
361   in panel a) between TNF-α versus PGI$_2$+TNFα EVs (p<0.05). (c) Western blot analyses of
362   distinct EV preparations used to detect immunoreactivity for Gelsolin (GSN), Annexin A1
363   (AnxA1), heat shock protein β1 (HSPB1) and β-actin (ACTB1). Three distinct EV
364   preparations were tested. (d) Densitometry analysis, ACTB1 was used as loading control. (e)
365   ImageStream™ analysis of a select group of proteins identified in the proteomic screen (see
366   Methods for details).   (f) Expression levels of GSN and ANXA1 in CD14+ EVs. *p<0.05,
367   **p<0.01, ***p< 0.001; Mann Whitney test, mean ± SEM, n=3 distinct EV preparations.

368

369   To determine the cell source of these exemplar proteins, surface staining and

370   intracellular staining of human monocytes and platelets aggregates was performed

371   by microscopy. While ANXA1 was selectively expressed, to a high abundance, by

372   monocytes (Fig. 7a,b), the majority of GSN seemed to be expressed by platelets

373   both intracellularly and on their cell surface (Fig. 7a,b), while only a small amount

374   was associated to monocytes likely because adherent to platelets. Similar results

375   were also shown by Western blot when the same proteins were investigated in

376   platelet or monocyte (the latter containing residual platelets) lysates. Loading of

377 decreasing concentrations of monocyte and platelet whole lysates revealed GSN to

378 be highly expressed in platelets, and as described by the immunofluorescence

379 results, only a small amount of it was detected in the monocyte lysates possibly

380 because of platelet contamination (Fig 7c). Conversely, monocyte lysates contained

381 a consistent higher amount of ANXA1 represented by both the 38kDa and the 34kDa

382 bands (Fig 7c). Interestingly, platelet extracts displays only minimal amounts of the

383 cleaved form of ANXA1 (Fig 7d).

384 **Figure 7. Selective expression of Annexin A1 (ANXA1) and Gelsolin (GSN) in human**
385 **monocytes and platelets.** The monocyte preparation, that contains platelet, was prepared
386 as in Figure 2. Cells were permeabilised or left intact prior to staining for ANXA1 and GSN,
387 prior to imaging. (a) Surface staining for ANXA1 (red) and GSN (green) in monocytes/
388 platelets aggregates. (b) Intracellular staining for ANXA1 (red) and GSN (green) in
389 monocytes/ platelets aggregates. DAPI counterstaining (blue) indicates cell nuclei.
390 Representative of three distinct cell preparations. Scale bar = 10 μm. (c) Western blot
391 analysis for ANXA1 and GSN in monocyte and platelet lysates. (d) Densitometry analysis,
392 ACTB1 was used as loading control. (*p<0.05, **p<0.01, ***p< 0.001, Mann Whitney test,
393 mean ± SEM of n=5 with different donor cells).
394

395 In supplementary Table S6 we compare our data with other previously published

396 proteomics data conducted on EVs from THP-1 cells (a surrogate of monocytes) and

397 platelets.

Discussion

399

400   In this study we provide evidence that monocyte/platelet-derived EVs are by and

401   large pro-inflammatory and can activate not only endothelial cells, but also the

402   atherosclerotic plaque, inferring a pathogenic role in *in vivo* settings. We further

403   identify some subtlety in relation to the mode of activation of the monocyte with

404   particular attention to the presence of an aggregated and/or adherent platelet. Using

405   a pharmacological approach to preferentially attenuate platelet reactivity, we could

406   produce EVs with a lower pathogenic impact, at least in the context of an

407   atherosclerotic plaque activation. These different outcomes were not related to

408   physicochemical features of the EVs but rather to their composition as indicated by

409   the proteomic analysis. Since transient aggregates between monocytes and platelets

410   can form in several settings of vascular inflammation, we propose that this inter-

411   cellular cross-talk can generate EVs which may extend the patho-physiological

412   relevance of this event. Clinical management with anti-platelet therapies may have

413   beneficial effects also through a modulation of the quality of EVs released from

414   monocytes.

415

416   Monocyte/platelet aggregates are a reported feature of vascular inflammation, being

417   identified in several pathological settings, both in man and experimental animals. As

418   an example, an experimental medicine study following kidney transplantation,

419   revealed that addition of a 4-week anti-platelet therapy to immunosuppressive drugs

420   reduced monocyte/platelet aggregates as well as several other markers of vascular

421   inflammation (24). These aggregates have also been reported in stroke (25) and in

422   heart failure (26). In heart failure, a specific subset of monocyte/platelet aggregates

423   was negatively correlated with better prognosis, indicating a direct or indirect role for

15

424 the aggregates in promoting sustained damage, or reduced repair, of the cardiac

425 tissue. Finally, circulating monocyte/platelet aggregates have been detected in

426 hypertension, where an independent predictor for their formation was systemic blood

427 pressure (27), and in coronary artery disease. In the latter condition,

428 monocyte/platelet aggregates increase in patients compared to healthy controls

429 (28,29), an increase quantified to be more than two-fold (30). In all these studies, the

430 pro-atherogenic properties of the aggregates has been suggested. Of interest,

431 whereas some of the studies summarised here proposed an initiating role of the

432 platelets (24,30), there is evidence in the context of coronary artery disease that

433 indicates monocyte activation as the inciting event, leading to the formation of these

434 aggregates (31).

435

436 In all cases, monocyte/platelet aggregates and more generally leukocyte/platelet

437 aggregates, are transient in their association and dissociation. As a relevant

438 example, Furman *et al* demonstrated that numbers of circulating monocyte/platelet

439 aggregates in patients with acute myocardial dysfunction were higher within the first

440 4 hours of acute coronary symptoms and gradually returned to basal values in the 4-

441 8 hour period post-infarct (32). In a longer prospective study about patients

442 undergoing elective coronary bypass surgery, the numbers and reactivity of

443 monocyte/platelet aggregates decreased to basal level after 3 months from surgery

444 (33). Thus we reasoned that EVs could be represent a viable way to monitor longer-

445 term effects of aggregates formation, either as a biomarker or as *bona fide* effectors

446 of pathogenesis. As such we took advantage of the presence of platelets in the

447 preparations of monocytes purified from human whole blood. A subtle and

448 sophisticated role for the platelet emerged in these experimental conditions, whereby

449 attenuation of platelet activation with the prostacyclin analogue did not affect

450 platelets adhesion to the monocyte, while reducing the generation of EVs. In parallel

451 experiments, we used PAF. This stimulus activated preferentially the platelet,

452 produced a much larger number of EVs and specifically of CD41+ EVs: all these

453 effects were significantly inhibited by prostacyclin. This set of results validated our

454 conclusion that Iloprost acted predominantly on the platelet, yet it was able to affect

455 EVs when a myeloid cell stimulus like TNF-α was applied. Monitoring cytokines

456 released from the monocytes unveiled the inhibitory effect of the Iloprost which

457 added further substance to this conclusion. Altogether we have a system where with

458 TNF-α, we stimulate the monocyte predominantly, but there is a 'co-stimulatory'

459 action attained by the adherent platelets. These data are in agreement with a

460 proposed cross-talk in plaque formation and progression, whereby the platelet

461 adherent to the monocyte favours migration of the leukocyte into the plaque, which

462 would then develop to macrophages (34–36). Platelet-delivery of cholesterol could

463 feed forward the process of macrophage differentiation into a foam cells (37). Here

464 we reasoned that one downstream result of platelet/monocyte aggregate formation

465 would be production of pro-inflammatory EVs.

466

467 When EVs generated from the different *in vitro* incubation protocols were analysed

468 by Nanosight™ a relatively similar size was measured, with no major differences in

469 median and mode of the distribution when TNF-α or PAF were applied as stimuli, in

470 the presence or absence of prostacyclin analogue. In all cases, an average diameter

471 of >100 nm was quantified suggesting that EVs produced are predominantly formed

472 by membrane-spawn vesicles and not by exosomes (23). This evidence was

473 corroborated by the proteomic analysis and further validated by Western blot, which

474 identified ANXA1 in all subsets of EVs, with no significant changes across the

475 groups. A recent elegant study identified ANXA1 as a genuine marker for

476 membrane-spawn vesicles, also referred to as microparticles (23). More interesting

477 to us is the emerging evidence that the same cell can generate EVs which are at

478 least in part different in relation to the stimulus applied or the microenvironment. Our

479 own work on neutrophil-derived EVs reported major functional differences between

480 EVs produced in suspension versus in adhesion settings, with the former being

481 reparative and anti-inflammatory (Dalli et al. 2013; Headland et al. 2015) while the

482 latter EVs are mainly pro-inflammatory (6,39). In line with this, in this study, we could

483 demonstrate that monocyte-derived EVs isolated from mixed platelet/monocyte

484 aggregates in inflammatory conditions (TNF-α) bind to and are internalized by

485 HUVECs. Importantly, EVs isolated from TNF-α treated monocyte/platelet

486 aggregates, but not from untreated cells or from cells previously treated with Iloprost,

487 up-regulated ICAM-1 and VCAM-1 expression and increased the release of GM-

488 CSF, IL-8 and IL-6 from endothelial cell monolayers. Before exploring further the

489 differences in composition we further tested the potential different effector functions

490 of TNF-α and Iloprost+TNF-α EVs using an organ culture protocol. For all the

491 reasoning summarised above we focused on the atherosclerotic plaque.

492

493 There has been quite some interest in EVs and atherosclerosis, mainly with a focus

494 on vesicles released from the plaque, possibly as a downstream determinant of

495 pathogenic processes operative within the plaque. Several studies showed that EVs

496 are mainly derived from leukocytes and i) are endowed with thrombogenic activities

497 (40), ii) can increase intra-plaque neovascularization and plaque vulnerability, mainly

498 iii) because they enhance proliferation of endothelial cells and angiogenesis (41)

499   through the presence of tissue factor activity (42). The leukocyte origin was further

500   confirmed by Mayr *et al*, using a combination of unbiased analyses to quantify and

501   qualify the myeloid EV fraction, as well as EVs from smooth muscle cells and

502   erythrocytes. Metabolomics performed in the same study showed an increase in

503   taurine, further emphasizing the monocyte/neutrophil-produced oxidative

504   microenvironment within the atherosclerotic plaque (14). Here we revealed marked

505   modulatory functions of monocyte EVs applied to the plaque. After 24 h incubation,

506   the plaque was relatively viable as assessed with both focused and unbiased

507   approaches, the former being multiple cytokine quantifications, the latter proteomic

508   analysis, both conducted on plaque supernatants. The induction of several cytokines

509   by TNF-α EVs is indicative of strong pro-inflammatory actions supporting the

510   hypothesis that if generated within the plaque (perhaps from the extravasating

511   monocyte bearing platelets on its surface) or migrated to the plaque, these vesicles

512   can fuel local inflammatory processes. The increase in IL-6 is remarkable and fits

513   with several studies that identify the importance of this cytokine in the development

514   of atherosclerosis. Exogenously administered IL-6 significantly enhances (~5-fold)

515   the development of fatty lesions in mice (43). The pathogenic properties of IL-6

516   through enhancing endothelial dysfunction and aortic stiffness was demonstrated in

517   rheumatoid arthritis patients treated with the IL-6 receptor inhibitor tocilizumab: the

518   neutralizing anti-IL-6 therapy successfully reduced articular inflammation and

519   decreased endothelial dysfunction, measured as impaired flow mediated dilatation

520   and aortic stiffness by pulse wave velocity (44). A recent Mendelian randomized

521   study, focusing on the single nucleotide polymorphisms in the IL-6 receptor gene,

522   highlighted loss of function as a viable approach for the prevention of coronary heart

523   disease (45). It was of great interest to us that the vesicles generated by the

19

524 monocyte preparation stimulated with Iloprost+TNF-α displayed a totally different

525 impact on the plaque. The cytokine response of the plaque was essentially blunted

526 when compared to that quantified following overnight incubation with TNF-α EVs.

527

528 The fact that TNF-α EVs markedly affected the reactivity of ex vivo cultured

529 atherosclerotic plaque was further confirmed by proteomic analysis of the

530 conditioned media with the identification of a 52 significantly modulated proteins in

531 response to the different EVs subsets. In particular, the proteome of the plaque

532 conditioned media unveiled modulation of a different group of proteins between TNF-

533 α and Iloprost+TNF-α EVs with an important distinction. While TNF-α EVs

534 augmented ~3-fold the levels of fibulin-2 in the plaque supernatants, Iloprost+TNF-α

535 EVs failed to do so, indicating a head-to-head difference in line with the cytokine

536 analyses. Fibulin-2 is an extracellular matrix protein that has been positively

537 associated with fibrosis of the myocardium (46). In a model of heart failure, mice

538 nullified for fibulin-2 are less susceptible to fibrosis while developing hypertrophy to

539 the same extent as their wild type counterparts. Such an outcome is secondary to

540 transforming growth factor beta expression in the presence of fibulin-2, together with

541 potentiation of its signalling in target cells. Moreover, while selective expression of

542 this protein in the aortic arch vessels it is known already to be associated with the

543 morphogenic events that regulate heart development, in post-natal life fibulin-2 is

544 also produced by endothelial cells of the coronary arteries and veins (47). These

545 properties dovetail with the results obtained by our experiments whereby modulation

546 of fibulin-2 follows the inflammatory status of the plaque and the regulation afforded

547 by distinct types of EVs. Furthermore, the fact that fibulin-2 is required for higher

548 deposition of collagen-I and collagen-III in cardiac fibrosis corroborate the

549   pathogenic role that this protein may have in plaque formation and/or progression.

550   One would derive that strategies to modulate fibulin-2 levels within the plaque,

551   perhaps through delivery of antisense or blocking strategies with natural or semi-

552   synthetic vesicles (47,48), could be a viable therapeutic approach to impact on the

553   progression of atherosclerosis.

554

555   Finally, the experiments presented and discussed above justified an in-depth

556   analysis of the potential differences between TNF-α EVs and Iloprost+TNF-α EVs.

557   While we recognise that structural lipids, lipid mediator precursors (49), microRNA

558   and other nucleic acids (50) could vary between the two vesicle types, as a proof-of-

559   concept for fundamental differences in composition, we analysed their protein

560   contents. In general a lower number of significantly modulated proteins were

561   detected in Iloprost+TNF-α EVs compared to TNF-α EVs suggesting that attenuation

562   of platelet activation not only reduced the number of CD14+ and CD14/CD41+ EVs,

563   but also modified the actual composition of these microstructures. Addition of Iloprost

564   reduced the number of proteins exclusively identified in monocyte EVs from 10

565   proteins to 2. Comparison with published proteomic lists revealed interesting

566   overlaps. As an example, THP-1 monocytic cells stimulated with lipopolysaccharide

567   yield EVs that contain EEF1B2 (an elongation factor) and PSMC2 (proteasome

568   subunit) (51), two of the proteins uniquely identified here for TNFα EVs. Out of six

569   studies of platelet EVs, we focused on two studies (52,53) were similar preparation

570   protocols were applied for the generation of the EVs. Thus, INA (cytoskeleton

571   component) uniquely identified in Iloprost+TNF-α EVs was identified by Pienimaeki-

572   Roemer *et al.* in senescent platelet EVs (52). Platelet EVs also express PSMC2 as

573   well as AP2M1 (vesicle transporter) and PSMB6 (another proteasome subunit) (52).

574   Similar overlaps were noted for the proteins modulated in both subgroups of EVs

575   analysed here, as reported in Table S6. An interesting hit was gelsolin, detected in

576   more abundance in Iloprost+TNF-α EVs and also in plaques treated with this EV

577   subset: this protein is endowed with anti-inflammatory properties and has been

578   identified in resolving inflammatory exudates (54). In this study, addition of gelsolin to

579   chondrocytes exerted positive modulation of extracellular matrix protein deposition

580   while inhibiting metalloproteases and other catabolic enzymes. In the context of an

581   atherosclerotic plaque, such a profile would yield a stabilizing effect. In fact,

582   published data using proteomic approaches have reported gelsolin downregulation in

583   atherosclerotic coronary arteries compared to pre-atherosclerotic coronaries and

584   mammaries (55). The same authors demonstrated how reduction in gelsolin levels

585   caused i) cytoskeleton deregulation within the human atherosclerotic coronary media

586   layer and ii) switch of medial vascular smooth muscle cells from a contractile to a

587   synthetic phenotype (proinflammatory) (56). Furthermore, circulating levels of

588   gelsolin are reduced in patients with a diagnosis of asymptomatic carotid artery

589   plaque (57) and in patient with ankylosing spondylitis undergoing TNF-α antagonist-

590   infliximab therapy when compared to healthy matched controls (58).

591

592   Collectively these data strengthen the close relationship between monocytes and

593   platelets for the generation of EVs which may be of mixed origin, with proteins that

594   may derive from one cell or the other. As such future studies may focus on the

595   biogenesis of EVs from the aggregates and perhaps reveal a common budding

596   process into the vesicles that emerge from them.

597

598   In conclusion, the activating effect of monocyte-derived vesicles on the reactivity of

599   the atherosclerotic plaque reflects the contribution of platelet adhesion.

600   Monocyte/platelet aggregates, accepted as a predictive marker of several

601   cardiovascular pathologies including coronary artery disease, may have longer

602   lasting pathogenic effects through generation of vesicles which may propagate pro-

603   inflammatory actions. Modulation of platelet reactivity could help attenuating the

604   detrimental properties of these vesicles.

605

606   **Material and methods.**

607   <u>Monocyte purification and flow cytometry characterization.</u> All volunteers gave

608   written, informed consent to blood collection and the procedure was approved by the

609   Queen Mary Ethics of Research Committee (QMERC2014.61) for healthy controls.

610   Blood (30 ml) was drawn from healthy volunteers using a 19G butterfly needle with

611   tourniquet applied and anticoagulated with 0.32% w/v sodium citrate. To inhibit

612   platelet activation, Iloprost™ (2µM; stable prostacyclin analogue; Sigma-Aldrich,

613   Gillingham, UK) was added to whole blood prior cell separation. The blood was, then

614   centrifuged at 150 x*g* for 20 min and the platelet rich plasma (PRP) removed and

615   replaced with PBS+1mM EDTA. Following another centrifugation step, RosetteSep™

616   cocktail (15028, StemCell Technology, Vancouver, Canada) was added (50 µl/ml of

617   blood) and samples rested at room temperature for 20 mins. Blood was then diluted

618   1:1 with PBS+1mM EDTA and layered over 15 ml Histopaque 1077 (Sigma-Aldrich,

619   Gillingham, UK), centrifuged for 20 min at 1200 x*g* room temperature to separate

620   monocytes from other cells. The monocyte layer was harvested and washed at 300

621   x*g* for 10 min. Following another washing step, the monocyte pellet was re-

622   suspended in phenol red-free RPMI (Gibco, Waltham, US) and the concentration

623   adjusted as needed.

624

625   For peripheral blood mononuclear cells (PBMCs) isolation, whole blood was

626   centrifuged at 130 ×*g* for 20 minutes and plasma was removed. For every 30 ml of

627   whole blood, erythrocytes were depleted by sequentially layering 10 ml PBS followed

628   by 8 ml of 6% w/v dextran (high molecular weight, Sigma-Aldrich, in PBS) and gently

629   inverting. After 15 min, the leukocyte-rich fraction was collected and layered over

630   Histopaque 1077 and centrifuged for 30 minutes 450 x*g* at room temperature to

631   separate granulocytes from PBMC. PBMCs were washed once by centrifuging at

632   300 ×*g* and resuspended in RPMI for further use. For polymorphonuclear cells

633   (PMN) isolation, whole blood was centrifuged at 130 x*g* for 20 min, plasma removed,

634   erythrocytes depleted on 6% w/v dextran (high molecular weight, Sigma-Aldrich, in

635   PBS). Then, the leukocyte-rich fraction was layered over Histopaque and centrifuged

636   for 30 min 450 x*g* at room temperature. The PMN layer was harvested, washed and

637   cell concentration adjusted as needed.

638   After isolation cells were treated with Fc receptor blocking solution and stained with

639   anti-CD14-APC (2 µg/ml, 61D3; Biolegend, San Diego, USA), anti-CD41-PE

640   (2 µg/ml, HIP8; Biolegend), anti P-selectin-FITC or anti-PSGL1-PE (2.5 and 1.5

641   µg/ml, AC1.2 and KLP-1 respectively; Becton Dikinson, Franklin Lakes, USA). Cells

642   were acquired on an LSR Fortessa cytometer.

643

644   For platelet isolation, PRP was isolated directly from blood by centrifugation as

645   above. PRP was further processed into washed platelets (WP) by addition of 2µg/ml

646   Iloprost and 0.02U/ml apyrase (M0398S, NEB), prior to centrifugation at 1000 *xg* for

647 10 minutes. Pellets were re-suspended in modified HEPES Buffer containing Iloprost

648 and apyrase and washed a second time. Platelet where then counted, and

649 concentration was adjusted to 3×10^8/mL before stimulating.

650

651 <u>Fluorescent microscopy analysis of monocytes and platelets.</u> Isolated monocytes

652 containing platelets were spotted on Alcian blue-coated glass slides and fixed in cold

653 4% paraformaldehyde (4 °C, 30 min). After fixation, cells were washed with PBS and

654 then blocked in PBS with 0.2% BSA (for surface staining) or PBS with 0.1% Triton

655 and 0.2% BSA (T-PBS; for intracellular staining) for 30 min at room temperature

656 shaking. Following blocking, monocytes and platelets were incubated with primary

657 specific antibodies against Annexin A1 (ANXA1; 5 µg/ml; clone 1B, in house

658 generated) and Gelsolin (GSN; 1.54 µg/ml clone EPR1942; Abcam, Cambridge, UK)

659 in either PBS+0.2% BSA or T-PBS+0.2% BSA overnight at 4 °C. The cells were then

660 washed and incubated with secondary antibody Alexa Fluor 488 anti-rabbit (5 µg/ml,

661 Molecular Probes Invitrogen, Eugene, USA) or Alexa Fluor 592 anti-mouse (5 µg/ml,

662 Molecular Probes Invitrogen) in T-PBS+0.2% BSA for 1 h at 20 °C shaking. Cells

663 were then mounted with a glass coverslip using Fluoroshield™ Histology Mounting

664 Medium with DAPI (Sigma-Aldrich) and visualized under the microscope Zeiss

665 LSM800 Imaging System.

666

667 <u>Western blot analysis of monocytes and platelets.</u> Presence GSN and ANXA1 was

668 confirmed through standard SDS-PAGE (Millipore, Watford, UK), loading extracts

669 from 30µg, 10 µg, 3µg and 1 µg of isolated monocyte or washed platelet lysates.

670 Western blot was conducted with specific antibodies against ANXA1 (ANXA1; 5

671 ng/ml; clone 1B), GSN (1.54 ng/ml clone EPR1942; Abcam, Cambridge, UK), or

672   anti-β-actin (ACTB; 5 ng/ml; clone AC-74, Sigma-Aldrich) overnight at 4 °C followed

673   by a 1 h incubation with either an HRP-conjugated goat anti-mouse IgG or goat anti-

674   rabbit IgG (Dako, Cambridge, UK). Proteins were detected using Luminata™ Forte

675   Western HRP Substrate (Millipore, Watford, UK) visualized on Hyperfilm™ (GE

676   Healthcare, Buckinghamshire, UK).

677

678   <u>Generation and isolation of monocyte EVs.</u>   Monocytes (1×10^6 cells/mL) were

679   incubated with TNF-α (50 ng/mL; Sigma-Aldrich), platelet activator factor (PAF, 1 μM;

680   Cayman Chemical, Ann Arbor, USA) or PBS for 60 min at 37°C. Washed platelets

681   were incubated with 50 ng/mL TNF-α for 20 min at 37°C. When the prostacyclin

682   analogue Iloprost was added, it was used at 1 μM (Iloprost®; Sigma-Aldrich). Cell

683   suspensions were centrifuged at 4,400 x*g* at 4°C for 15 min to pellet cells and/or

684   platelets, followed by a second centrifugation at 13,000 x*g* at 4°C for 2 min to remove

685   remaining contaminants (e.g. apoptotic bodies). EVs were enriched by centrifuging

686   at 20,000 x*g* at 4°C for 30 min, the supernatant was removed, and pellets were re-

687   suspended in filtered sterile PBS.

688

689   <u>Characterization of monocyte-derived EVs.</u>

690   *Nanoparticle tracking analysis for sizing EVs.* Approximately 0.5 ml of EVs

691   (between 10^6 to 10^8 vesicles) in suspension were loaded onto the Nanosight NS300

692   with 488 nm scatter laser and high sensitivity camera (Malvern Instruments Ltd.,

693   Malvern, UK); five videos of 90 seconds each were recorded for each sample. Data

694   analysis was performed with NTA2.1 software (Nanosight, Malvern, UK). Software

695   settings for analysis were the following, Detection Threshold: 5–10; Blur: auto;

696   Minimum expected particle size: 20 nm.

697 *ImageStream™ analysis for quantification and characterisation of EVs.* EVs were

698 analysed and counted using fluorescence triggering on an ImageStreamx™ MKII

699 imaging cytometer as described previously (Headland et al. 2015). Briefly, vesicles

700 were labelled with 50 µM BODIPY maleimide fluorescein or BODIPY Texas-Red (Life

701 Technologies, Carlsbad, USA), and acquired as such or after labelling with either

702 2 µg/ml anti-CD14-APC (61D3; Biolegend), 2 µg/ml anti-CD41-PE (HIP8; Biolegend)

703 or one of the following Pacific Blue or Alexa Fluor 488 conjugated antibodies: anti-

704 Annexin A1 (ANXA1; 1 µg/ml; clone 1B), anti-Gelsolin (GSN; 0.1 µg/ml clone

705 EPR1942; Abcam). Fluorescence minus one (FMO) controls were used for gating all

706 protein antigen-positive events. Approximately 20,000 events were acquired per

707 sample.

708 *Proteomic analysis of EVs.* EVs derived from monocytes treated with TNFα in

709 presence or absence of Iloprost® were pelleted at 20,000 *xg* for 30 min,

710 resuspended in 20 µl ice cold RIPA buffer containing protease inhibitor (Sigma

711 Aldrich). Protein content was measured by spectrophotometry (Nanodrop 2000,

712 ThermoFisher Scientific, Waltham, USA) selecting Protein A280 program and 50 µg

713 of proteins were used for trypsin digestion. Mass spectrometry analysis of the

714 proteins obtained from EVs was performed on tryptic digests obtained using the

715 Filter Aided Sample Preparation protocol as previously described (59). EVs

716 proteome profile was determined by LC-MS/MS analysis as previously described in

717 the methods section All data and materials have been made publicly at the PRIDE

718 (60) Archive (EMBL-EBI) with the dataset identifier PXD014325.

719 *Western blotting analyses.* Presence of a select group of proteins identified by

720 proteomic analysis was confirmed through standard SDS-PAGE, loading extracts

721 from ~30 × 10^6 EVs per lane (Millipore, Watford, UK). Western blot was conducted

722 with specific antibodies against ANXA1 (ANXA1; 5 µg/ml), GSN (1.54 µg/ml clone

723 EPR1942; Abcam), anti-Heat shock protein β-1 (HSPB1; 5 µg/ml; clone G3.1;

724 Abcam), or anti-β-actin (ACTB; 5 µg/ml; clone AC-74, Sigma-Aldrich) overnight at 4

725 °C followed by a 1 h incubation with either an HRP-conjugated goat anti-mouse IgG

726 or goat anti-rabbit IgG (Dako). Proteins were detected using Luminata™ Forte

727 Western HRP Substrate (Millipore) visualized on Hyperfilm™ (GE Healthcare).

728

729 <u>Experiments with Human Umbilical Vein Endothelial Cells (HUVEC)</u>.

730 *Isolation and culturing of HUVEC.* Cells were freshly isolated from umbilical cords

731 that were kindly donated by the midwifery staff of the Maternity Unit, Royal London

732 Hospital (London, UK) with an approved protocol (East London & The City Local

733 Research Ethics Committee reference 05/Q0603/34 ELCHA). Cells were cultured

734 0.5% gelatin coated T75 flasks, in 5% CO_2 at 37°C with complete Medium 199

735 (Gibco, Waltham, USA) containing 100 U penicillin, 100 mg/mL streptomycin, and

736 2.5 µg/mL fungizone (Gibco) supplemented with 20% Human serum (Sigma-Aldrich,

737 UK), and used up to passage 4.

738 *Assessment of adhesion molecule expression by flow cytometry.* HUVEC were

739 grown to confluence in 6 well plate coated with 0.5% gelatin and stimulated 24 hours

740 with TNF-α (10 ng/mL), or $10x10^6$ EVs isolated from monocyte-platelet aggregates

741 subsequent to stimulation with vehicle, TNF-α, or iloprost+TNF-α, in 0.5% human

742 serum complete media, as described above. After isolation cells were treated with

743 Fc receptor blocking solution and stained with anti-ICAM-1- PE (1 µg/ml, HA58;

744 Biolegend, San Diego, USA), anti-VCAM-1- BV711 (0.5 µg/ml, 5110C9; Optibuilt,

745 USA). Cells were acquired on an LSR Fortessa cytometer.

746   *Confocal imaging of EV uptake.* HUVEC were seeded overnight on 0.5% Gelatin

747   coated μ-Slide 8 Well Glass Bottom (80826, Ibidi) at a concentration of 1×10^5. Cells

748   were stimulated with 1×10^6 EV previously stained with 2.5 μM BODIPY-FITC for 20

749   min and pelleted at 20,000 *xg* for 30 minutes at 4ºC. Subsequently, the cells were

750   fixed with 4% PFA for 15 min and blocked and permeabilised with PBS containing

751   2% BSA and 0.1% Triton-X for one hour. Cells were finally stained with 1.5 nM

752   Phalloidin AF647 (A22287, ThermoFisher Scientific) for 45 minutes. A Nanoimager-S

753   microscope (ONI, UK) was used for microscopy of the HUVEC using ONI software.

754   The following excitation/emission conditions were used in conjunction with x100

755   magnification oil immersion objectives: BODIPY 488/561 and AF647 640/658. The

756   images acquired were analysed using supplied ONI and ImageJ software packages.

757   Distinct BODIPY fluorescent (green) points identified by eye in the micrographs were

758   considered as distinct EV.

759

760   <u>Experiments with the human atherosclerotic plaque.</u>

761   *Isolation and ex vivo culture.* Patients with clinical and angiographic evidence of

762   atherosclerosis undergoing revascularization surgery were recruited to the study. All

763   5 patients undergoing carotid or femoral endarterectomy gave written informed

764   consent. The study was approved by the Ethics Committee of St. Vincent's

765   University Hospital in Dublin, and in accordance with the International guidelines and

766   Helsinki Declaration principles. Surgical atherosclerotic plaque samples were

767   harvested in physiological saline. After dissection, they were stimulated in 24-well

768   plates for 24 hours at 37°C, 5% CO_2 in RPMI with 0.1% exosome depleted Fetal

769   Bovine Serum with the different EV subsets (10×10^6 per well), which were isolated

770   from monocyte-platelet aggregates subsequent to stimulation with vehicle, TNF-α, or

771 iloprost+TNF-α as described above. After 24 hr incubation, tissues samples and

772 supernatants were collected and snap frozen in liquid nitrogen for subsequent

773 analysis by mass spectrometry analysis and multiplex ELISA assay.

774 *Proteomic analysis of plaque supernatants.* Conditioned media obtained from

775 plaque supernatants (from plaques treated with or without EVs, n=5) was defrosted

776 at room temperature and centrifuged firstly at 14,000 x*g* for 2 min to remove debris

777 and then at 20,000 x*g* at 4°C to remove residual EVs from both the stimulation and

778 the exosome depleted FBS, this sequential centrifugation reduced further ~94% the

779 number of EV contained in the FBS. An equal volume of 20% trichloroacetic acid

780 was added to the sample and incubated on ice for 1 hr. Samples were centrifuged at

781 10,000 x*g* for 15 min at 4°C and washed with 500 µl of ice-cold acetone. After 5 min

782 incubation, proteins were spun for 5 min at 5,000 x*g* at 4°C, acetone was removed

783 and pellets were left to dry. Dried protein pellets were re-suspended in 8 M Urea/ 25

784 mM Tris– HCl, pH 8.2. Disulphide bonds were reduced with 5 mM Dithiothreitol

785 (DTT) and protected with 15 mM iodoacetamide. Proteins were digested with

786 sequencing grade trypsin (1:100; Promega, USA) overnight at 37°C and peptides

787 concentration was checked by spectrophotometry (Nanodrop 2000; ThermoFisher

788 Scientific, Waltham, USA). Then,15 µg of peptides were purified using ZipTipC18

789 pipette tips according to manufacturer's instructions (Millipore, Billerica, USA),

790 resuspended in 2% Acetonitrile/0.1% formic acid solution, prior to injection of 2 µg of

791 purified peptides into an Ultimate3000 nano-LC system coupled to a Q Exactive

792 mass spectrometer (ThermoFisher Scientific) for mass spectrometry. Peptides were

793 separated by increasing acetonitrile, 2 to 33%, in a linear gradient of 40 min on a

794 C18 reverse phase chromatography column packed with 2.4 µm particle size, 300 Å

795 pore size C18 material (Dr Maisch GmbH, Ammerbuch Entringen, Germany) to a

796 length of 120 mm in a column with a 75 µm, using a flow rate of 250 nL/min. All data

797 were acquired with the mass spectrometer operating in an automatic data dependent

798 acquisition mode (DDA, shotgun). A full mass spectrometry service scan at a

799 resolution of 70,000, AGC target 3e6 and a range of m/z 350–1600 was followed by

800 up to 12 subsequent MS/MS scan with a resolution of 17,500, AGC target 2e4,

801 isolation window m/z 1.6 and a first fix mass of m/z 100. Dynamic exclusion was set

802 to 40 s. Mass spectrometry data were processed using label-free quantitation

803 method in MaxQuant software v.1.3.0.547, using the human Uniprot database

804 (release 2016_3). All data and materials have been made publicly available at the

805 PRIDE Archive (EMBL-EBI)(60) partner repository with the dataset identifier

806 PXD014324.

807

808 Downstream analysis of proteomic data was performed by Perseus software (version

809 1.6.0.7). Only the proteins present in at least 50% of the samples in at least one

810 group ("Untreated" plaque, "TNF-α", "PGI$_2$", "TNF-α+PGI$_2$ EVs treated plaque) were

811 considered identified. Proteins found to be differentially expressed between groups

812 (Student's T-test P<0.05, FDR 0.05) were subjected to enrichment analysis and were

813 distributed into categories according to cellular component, molecular function,

814 biological process, KEEG pathways and reactome pathways using PANTHER

815 (Version 14.1) or STRING Database (Version 10.5). STRING was also used to

816 generate protein-protein interaction networks.

817 *Multiplex ELISA analysis of plaque and monocyte supernatants.*   GM-CSF,   IL-6

818 and IL-8 concentrations from HUVEC conditioned media or GM-CSF, IFN-γ, IL-1β,

819 IL-4, IL-6, IL-10, IL-13, MIP-1α and TNF-α concentrations from the centrifuged

820 conditioned media of the human plaques were measured by enzyme immunoassay

821 using commercially available human 96 well-plate multiplex kit for tissue culture

822 samples (MSD, Gaithersburg, USA) according to the manufacturers' guidelines. The

823 same cytokines plus MCP-1 instead of TNFα were quantified in the monocyte

824 conditioned media following removal of EVs by centrifugation.

825

826 <u>Statistical analysis.</u> All statistical analysis and graphing were performed in

827 GraphPad Prism 6 Software, IDEAS 6.2 for Image Stream Plots and FlowJo V6 for

828 LSRFortessas Plots. Data are expressed as mean ± standard error (SEM) unless

829 stated differently. Analyses applied to the different experimental data are indicated

830 in each figure legend. A p value of < 0.05 was considered significant to reject the null

831 hypothesis.

832

833 **Data Availability**

834 Mass spectrometry proteomics analysis of monocyte-derived EVs: PRIDE

835 PXD014324 (http://www.ebi.ac.uk/pride/archive/projects/ PXD014324)

836

837 Mass spectrometry proteomic analysis of human plaque supernatant: PRIDE

838 PXD014325 (http://www.ebi.ac.uk/pride/archive/projects/ PXD014325).

839

840 **Acknowledgments.**

846   EVOluTION has received funding from the European Union's Horizon 2020

847   research and innovation programme under the Marie Sklodowska-Curie grant

848   agreement No. 675111 (S.O., M.P.). Wellcome Trust (programme 086867/Z/08/Z) to

849   M.P. The ImageStream™ used was funded by the Wellcome Trust (infrastructure

850   grant 101604/Z/13/Z). M.deG. is supported by an IRC Government of Ireland

851   postdoctoral fellowship (IRC GOIPD/2017/1060), E.P.B and C.G are supported by

852   Science Foundation Ireland grants 15/US/B3130 and 15/IA/3152 and a strategic

853   research award from JDRF NY, USA. This work has been facilitated by the National

854   Institute for Health Research Biomedical Research Centre at Barts Hospital NHS

855   Trust.

856

857   **Author contributions**

858   M.P. devised the project, the main conceptual idea and proof outline. S.O. planned

859   the project, designed and performed experiments, analysed the data. C.G., helped

860   supervise the project, designed experiments, analysed the data; D.C. and L.V.N.

861   designed experiments, analysed the data. M. deG. and E.P.B assisted with *ex vivo*

862   atherosclerotic plaque experiments and S.M. helped carry out the proteomic

863   determinations and analyses. T.M.M. helped with the interpretation of the proteomic

864   data. M.B. helped providing the human samples used in the study. S.O. and M.P.

865   wrote the manuscript.

866

867   **Conflict of interest:**

868   None.

869

870

References

871

872 1. Hargett LA, Bauer NN. On the Origin of Microparticles: From "Platelet Dust" to

873   Mediators of Intercellular Communication. Pulm Circ. 2013;3(2):329–40.

874 2. Johnstone RM, Adam M, Hammond JR, Orr L, Turbide C. Vesicle formation

875   during reticulocyte maturation. Association of plasma membrane activities with

876   released vesicles (exosomes). J Biol Chem. 1987;262(19):9412–20.

877 3. Raposo G. B lymphocytes secrete antigen-presenting vesicles. J Exp Med.

878   1996;183(3):1161–72.

879 4. Pucci F, Garris C, Lai CP, Newton A, Pfirschke C, Engblom C, et al. SCS

880   macrophages suppress melanoma by restricting tumor-derived vesicle-B cell

881   interactions. Science (80-). 2016;352(6282):242–6.

882 5. Wei H, Malcor J-DM, Harper MT. Lipid rafts are essential for release of

883   phosphatidylserine-exposing extracellular vesicles from platelets. Sci Rep.

884   2018 Dec 3;8(1):9987.

885 6. Dalli J, Montero-Melendez T, Norling L V, Yin X, Hinds C, Haskard D, et al.

886   Heterogeneity in Neutrophil Microparticles Reveals Distinct Proteome and

887   Functional Properties. Mol Cell Proteomics. 2013 Aug;12(8):2205–19.

888 7. Giebel B. On the function and heterogeneity of extracellular vesicles. Ann

889   Transl Med. 2017 Mar;5(6):150.

890 8. Holnthoner W, Bonstingl C, Hromada C, Muehleder S, Zipperle J, Stojkovic S,

891   et al. Endothelial Cell-derived Extracellular Vesicles Size-dependently Exert

892   Procoagulant Activity Detected by Thromboelastometry. Sci Rep. 2017 Dec

893   16;7(1):3707.

894 9. Jansen F, Yang X, Hoyer FF, Paul K, Heiermann N, Becher MU, et al.

895   Endothelial   Microparticle   Uptake   in   Target   Cells   Is   Annexin

896   I/Phosphatidylserine Receptor Dependent and Prevents Apoptosis.

897   Arterioscler Thromb Vasc Biol. 2012 Aug;32(8):1925–35.

898   10. Collier MEW, Ettelaie C. Induction of Endothelial Cell Proliferation by

899   Recombinant and Microparticle-Tissue Factor Involves β1-Integrin and

900   Extracellular Signal Regulated Kinase Activation. Arterioscler Thromb Vasc

901   Biol. 2010 Sep;30(9):1810–7.

902   11. Wilkins E, L. W, Wickramasinghe K, P B. European Cardiovascular Disease

903   Statistics 2017. Eur Hear Netw. 2017;

904   12. Moore KJ, Tabas I. Macrophages in the pathogenesis of atherosclerosis. Cell.

905   2011;145(3):341–55.

906   13. Jansen F, Li Q, Pfeifer A, Werner N. Endothelial- and Immune Cell-Derived

907   Extracellular Vesicles in the Regulation of Cardiovascular Health and Disease.

908   Vol. 2, JACC: Basic to Translational Science. 2017. p. 790–807.

909   14. Mayr M, Grainger D, Mayr U, Leroyer AS, Leseche G, Sidibe A, et al.

910   Proteomics, Metabolomics, and Immunomics on Microparticles Derived From

911   Human Atherosclerotic Plaques. Circ Cardiovasc Genet. 2009 Aug;2(4):379–

912   88.

913   15. Hoyer FF, Giesen MK, Nunes França C, Lütjohann D, Nickenig G, Werner N.

914   Monocytic microparticles promote atherogenesis by modulating inflammatory

915   cells in mice. J Cell Mol Med. 2012;16(11):2777–88.

916   16. Headland SE, Jones HR, D'Sa AS V., Perretti M, Norling L V. Cutting-Edge

917   Analysis of Extracellular Microparticles using ImageStreamX Imaging Flow

918   Cytometry. Sci Rep. 2015 May 10;4(1):5237.

919   17. Wang J-G, Williams JC, Davis BK, Jacobson K, Doerschuk CM, Ting JP-Y, et

920   al. Monocytic microparticles activate endothelial cells in an IL-1β-dependent

921   manner. Blood. 2011 Aug 25;118(8):2366–74.

922   18.   Kuravi SJ, Harrison P, Rainger GE, Nash GB. Ability of Platelet-Derived
923   Extracellular Vesicles to Promote Neutrophil-Endothelial Cell Interactions.
924   Inflammation. 2019 Feb 14;42(1):290–305.

925   19.   Dalvi P, Sun B, Tang N, Pulliam L. Immune activated monocyte exosomes
926   alter microRNAs in brain endothelial cells and initiate an inflammatory
927   response through the TLR4/MyD88 pathway. Sci Rep. 2017 Dec 30;7(1):9954.

928   20.   Aharon A, Tamari T, Brenner B. Monocyte-derived microparticles and
929   exosomes induce procoagulant and apoptotic effects on endothelial cells.
930   Thromb Haemost. 2008 Nov;100(5):878–85.

931   21.   Tang N, Sun B, Gupta A, Rempel H, Pulliam L. Monocyte exosomes induce
932   adhesion molecules and cytokines via activation of NF-κB in endothelial cells.
933   FASEB J. 2016;30(9):3097–106.

934   22.   Sun HQ, Yamamoto M, Mejillano M, Yin HL. Gelsolin, a Multifunctional Actin
935   Regulatory Protein. J Biol Chem. 1999 Nov 19;274(47):33179–82.

936   23.   Jeppesen DK, Fenix AM, Franklin JL, Higginbotham JN, Zhang Q, Zimmerman
937   LJ, et al. Reassessment of Exosome Composition. Cell. 2019 Apr;177(2):428-
938   445.e18.

939   24.   Graff J, Harder S, Wahl O, Scheuermann EH, Gossmann J. Anti-inflammatory
940   effects of clopidogrel intake in renal transplant patients: Effects on platelet-
941   leukocyte interactions, platelet CD40 ligand expression, and proinflammatory
942   biomarkers. Clin Pharmacol Ther. 2005;78(5):468–76.

943   25.   Franks ZG, Campbell RA, Weyrich AS, Rondina MT. Platelet-leukocyte
944   interactions link inflammatory and thromboembolic events in ischemic stroke.
945   Ann N Y Acad Sci. 2010 Oct;1207:11–7.

946 26. Wrigley BJ, Shantsila E, Tapp LD, Lip GYH. Increased Formation of monocyte-
947   platelet aggregates in ischemic heart failure. Circ Hear Fail. 2013;6(1):127–35.

948 27. Gkaliagkousi E, Corrigall V, Becker S, De Winter P, Shah A, Zamboulis C, et
949   al. Decreased platelet nitric oxide contributes to increased circulating
950   monocyte-platelet aggregates in hypertension. Eur Heart J. 2009;30(24):3048–
951   54.

952 28. Czepluch FS, Kuschicke H, Dellas C, Riggert J, Hasenfuss G, Schäfer K.
953   Increased proatherogenic monocyte-platelet cross-talk in monocyte
954   subpopulations of patients with stable coronary artery disease. J Intern Med.
955   2014;275(2):144–54.

956 29. Sarma J, Laan CA, Alam S, Jha A, Fox KAA, Dransfield I. Increased platelet
957   binding to circulating monocytes in acute coronary syndromes. Circulation.
958   2002;105(18):2166–71.

959 30. Furman MI, Benoit SE, Barnard MR, Valeri CR, Borbone ML, Becker RC, et al.
960   Increased Platelet Reactivity and Circulating Monocyte-Platelet Aggregates in
961   Patients With Stable Coronary Artery Disease. J Am Coll Cardiol. 1998;31(2).

962 31. Jurk K, Ritter MA, Schriek C, Van Aken H, Droste DW, Ringelstein EB, et al.
963   Activated monocytes capture platelets for heterotypic association in patients
964   with severe carotid artery stenosis. Thromb Haemost. 2010;103(6):1193–202.

965 32. Furman MI, Barnard MR, Krueger LA, Fox ML, Shilale EA, Lessard DM, et al.
966   Circulating monocyte-platelet aggregates are an early marker of acute
967   myocardial infarction. J Am Coll Cardiol. 2001 Oct;38(4):1002–6.

968 33. Ivert T, Dalén M, Ander C, Stålesen R, Lordkipanidzé M, Hjemdahl P.
969   Increased platelet reactivity and platelet–leukocyte aggregation after elective
970   coronary bypass surgery. Platelets. 2018 Nov 13;1–7.

34. Huo Y, Schober A, Forlow SB, Smith DF, Hyman MC, Jung S, et al. Circulating activated platelets exacerbate atherosclerosis in mice deficient in apolipoprotein E. Nat Med. 2003;9(1):61–7.

35. da Costa Martins P, van den Berk N, Ulfman LH, Koenderman L, Hordijk PL, Zwaginga JJ. Platelet-Monocyte Complexes Support Monocyte Adhesion to Endothelium by Enhancing Secondary Tethering and Cluster Formation. Arterioscler Thromb Vasc Biol. 2004 Jan;24(1):193–9.

36. Passacquale G, Vamadevan P, Pereira L, Hamid C, Corrigall V, Ferro A. Monocyte-Platelet Interaction Induces a Pro-Inflammatory Phenotype in Circulating Monocytes. Xu Q, editor. PLoS One. 2011 Oct 12;6(10):e25595.

37. Badrnya S, Schrottmaier WC, Kral JB, Yaiw K-C, Volf I, Schabbauer G, et al. Platelets Mediate Oxidized Low-Density Lipoprotein–Induced Monocyte Extravasation and Foam Cell Formation. Arterioscler Thromb Vasc Biol. 2014 Mar;34(3):571–80.

38. Headland SE, Jones HR, Norling L V., Kim A, Souza PR, Corsiero E, et al. Neutrophil-derived microvesicles enter cartilage and protect the joint in inflammatory arthritis. Sci Transl Med. 2015 Nov 25;7(315):315ra190-315ra190.

39. Dalli J, Norling L V, Montero-Melendez T, Canova DF, Lashin H, Pavlov AM, et al. Microparticle alpha-2-macroglobulin enhances pro-resolving responses and promotes survival in sepsis. EMBO Mol Med. 2014 Jan;6(1):27–42.

40. Leroyer AS, Isobe H, Lesèche G, Castier Y, Wassef M, Mallat Z, et al. Cellular Origins and Thrombogenic Activity of Microparticles Isolated From Human Atherosclerotic Plaques. J Am Coll Cardiol. 2007 Feb;49(7):772–7.

41. Leroyer AS, Rautou P-E, Silvestre J-S, Castier Y, Lesèche G, Devue C, et al.

996   CD40 Ligand+ Microparticles From Human Atherosclerotic Plaques Stimulate

997   Endothelial Proliferation and Angiogenesis. J Am Coll Cardiol. 2008

998   Oct;52(16):1302–11.

999   42.   Morel O, Toti F, Bakouboula B, Grunebaum L, Freyssinet J-M. Procoagulant

1000   Microparticles: 'Criminal Partners' in Atherothrombosis and Deleterious

1001   Cellular Exchanges. Pathophysiol Haemost Thromb. 2006;35(1–2):15–22.

1002   43.   Huber SA, Sakkinen P, Conze D, Hardin N, Tracy R. Interleukin-6 Exacerbates

1003   Early Atherosclerosis in Mice. Arterioscler Thromb Vasc Biol. 1999

1004   Oct;19(10):2364–7.

1005   44.   Protogerou AD, Zampeli E, Fragiadaki K, Stamatelopoulos K, Papamichael C,

1006   Sfikakis PP. A pilot study of endothelial dysfunction and aortic stiffness after

1007   interleukin-6 receptor inhibition in rheumatoid arthritis. Atherosclerosis. 2011

1008   Dec;219(2):734–6.

1009   45.   Swerdlow DI, Holmes M V., Kuchenbaecker KB, Engmann JEL, Shah T, Sofat

1010   R, et al. The interleukin-6 receptor as a target for prevention of coronary heart

1011   disease: a mendelian randomisation analysis. Lancet. 2012

1012   Mar;379(9822):1214–24.

1013   46.   Khan SA, Dong H, Joyce J, Sasaki T, Chu M-L, Tsuda T. Fibulin-2 is essential

1014   for angiotensin II-induced myocardial fibrosis mediated by transforming growth

1015   factor (TGF)-β. Lab Investig. 2016 Jul 25;96(7):773–83.

1016   47.   Tsuda T, Wang H, Timpl R, Chu M-L. Fibulin-2 expression marks transformed

1017   mesenchymal cells in developing cardiac valves, aortic arch vessels, and

1018   coronary vessels. Dev Dyn. 2001 Sep;222(1):89–100.

1019   48.   Ji H, Chen M, Greening DW, He W, Rai A, Zhang W, et al. Deep Sequencing

1020   of RNA from Three Different Extracellular Vesicle (EV) Subtypes Released

1021   from the Human LIM1863 Colon Cancer Cell Line Uncovers Distinct Mirna-

1022   Enrichment Signatures. Chen C, editor. PLoS One. 2014 Oct

1023   17;9(10):e110314.

1024   49.   Norling L V., Spite M, Yang R, Flower RJ, Perretti M, Serhan CN. Cutting

1025   Edge: Humanized Nano-Proresolving Medicines Mimic Inflammation-

1026   Resolution and Enhance Wound Healing. J Immunol. 2011 May

1027   15;186(10):5543–7.

1028   50.   Guduric-Fuchs J, O'Connor A, Camp B, O'Neill CL, Medina RJ, Simpson DA.

1029   Selective extracellular vesicle-mediated export of an overlapping set of

1030   microRNAs from multiple cell types. BMC Genomics. 2012;13(1):357.

1031   51.   Bernimoulin M, Waters EK, Foy M, Steele BM, Sullivan M, Falet H, et al.

1032   Differential stimulation of monocytic cells results in distinct populations of

1033   microparticles. J Thromb Haemost. 2009;7(6):1019–28.

1034   52.   Pienimaeki-Roemer A, Kuhlmann K, Böttcher A, Konovalova T, Black A, Orsó

1035   E, et al. Lipidomic and proteomic characterization of platelet extracellular

1036   vesicle subfractions from senescent platelets. Transfusion. 2015

1037   Mar;55(3):507–21.

1038   53.   Aatonen MT, Öhman T, Nyman TA, Laitinen S, Grönholm M, Siljander PRM.

1039   Isolation and characterization of platelet-derived extracellular vesicles. J

1040   Extracell Vesicles. 2014 Jan 6;3(1):24692.

1041   54.   Kaneva MK, Greco K V., Headland SE, Montero-Melendez T, Mori P,

1042   Greenslade K, et al. Identification of Novel Chondroprotective Mediators in

1043   Resolving Inflammatory Exudates. J Immunol. 2017 Apr 1;198(7):2876–85.

1044   55.   de la Cuesta F, Barderas MG, Calvo E, Zubiri I, Maroto AS, Darde VM, et al.

1045   Secretome analysis of atherosclerotic and non-atherosclerotic arteries reveals

1046   dynamic extracellular remodeling during pathogenesis. J Proteomics. 2012

1047   Jun;75(10):2960–71.

1048   56.   de la Cuesta F, Zubiri I, Maroto AS, Posada M, Padial LR, Vivanco F, et al.

1049   Deregulation of smooth muscle cell cytoskeleton within the human

1050   atherosclerotic coronary media layer. J Proteomics. 2013 Apr;82:155–65.

1051   57.   Bhosale SD, Moulder R, Venäläinen MS, Koskinen JS, Pitkänen N, Juonala

1052   MT, et al. Serum Proteomic Profiling to Identify Biomarkers of Premature

1053   Carotid Atherosclerosis. Sci Rep. 2018 Dec 15;8(1):9209.

1054   58.   Genre F, López-Mejías R, Miranda-Filloy JA, Ubilla B, Carnero-López B,

1055   Gómez-Acebo I, et al. Gelsolin levels are decreased in ankylosing spondylitis

1056   patients undergoing anti-TNF-alpha therapy. Clin Exp Rheumatol.

1057   2014;32(2):218–24.

1058   59.   Wiśniewski JR, Zougman A, Nagaraj N, Mann M. Universal sample

1059   preparation method for proteome analysis. Nat Methods. 2009 May

1060   19;6(5):359–62.

1061   60.   Perez-Riverol Y, Csordas A, Bai J, Bernal-Llinares M, Hewapathirana S,

1062   Kundu DJ, et al. The PRIDE database and related tools and resources in

1063   2019: improving support for quantification data. Nucleic Acids Res. 2019 Jan

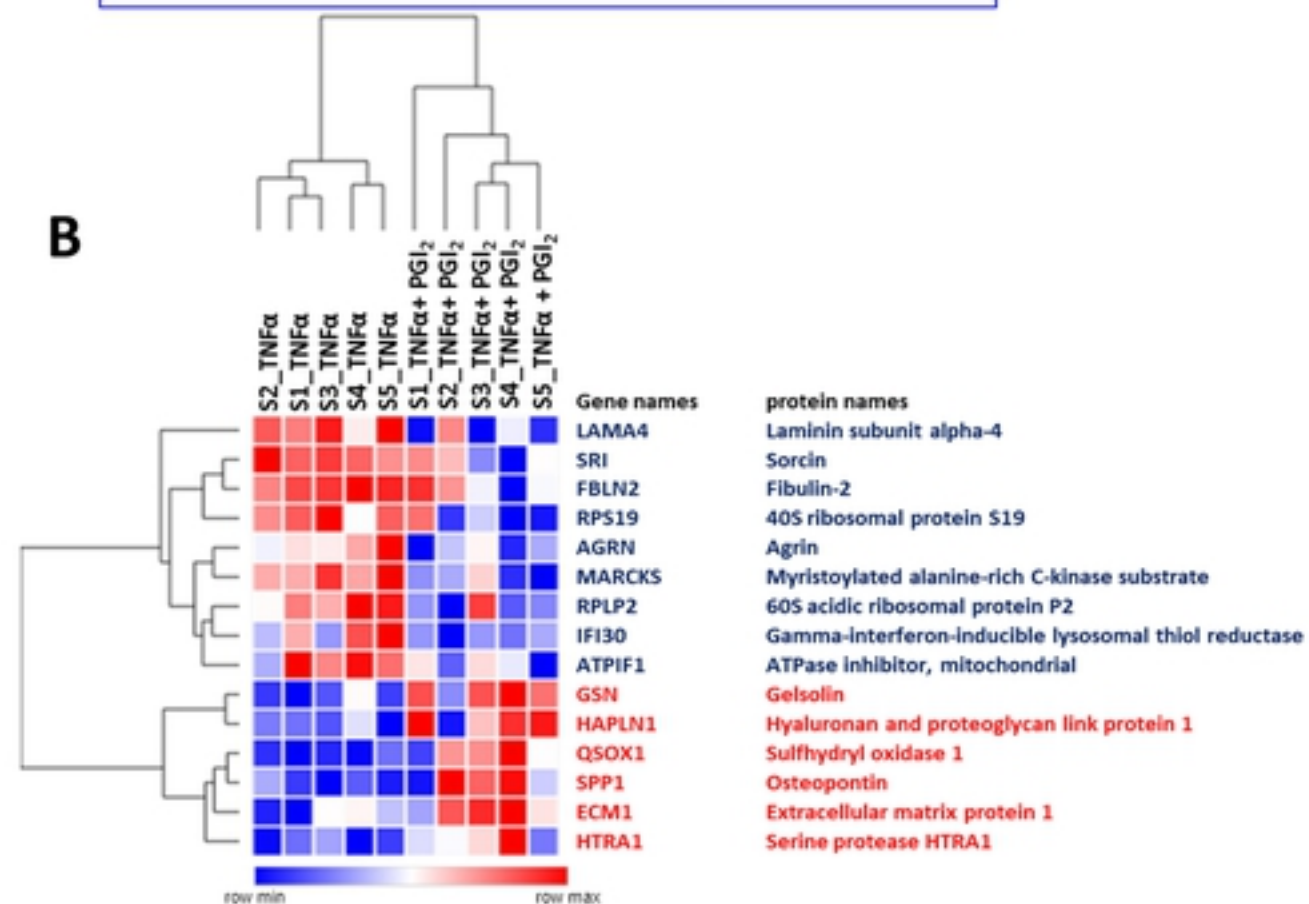1064   8;47(D1):D442–50.

1065

1066

1067

1068

1069

1070

1071

Fig1

Fig2

Fig3

Fig4

Fig5

Fig6

Fig7